Digest Journal of Nanomaterials and Biostructures Vol. 9, No. 3, July - September 2014, p. 1187 - 1197

SYNTHESIS, CHARACTERIZATION AND ADSORPTION STUDIES OF FLUORINE–DOPED CARBON NANOTUBES

A. O. OSIKOYA[a], D. WANKASI[a], R. M. K. VALA[a], A. S. AFOLABI[b], E. D. DIKIO[a*]
[a]*Applied Chemistry and Nanoscience Laboratory, Department of Chemistry, Vaal University of Technology, P. O. Box X021, Vanderbijlpark, South Africa*
[b]*Department of Civil and Chemical Engineering, College of Science, Engineering and Technology, University of South Africa, Private Bag X6, Johannesburg, South Africa*

Fluorine-doped carbon nanotubes were synthesized using cobalt and silver co-catalyst on magnesium oxide support and their morphological features studied using Raman spectroscopy, energy dispersive spectroscopy (EDX), scanning electron microscopy (SEM), transmission electron microscopy (TEM), and X-ray diffraction spectroscopy. The morphological images showed amorphous multiwall nanotubes with some crystalline regions that are attributable to the doping of the fluorine. The prepared material was used as adsorbent and the adsorption studies recorded a rapid uptake of Cr^{3+} by the CNTs which was mainly diffusion controlled. Equilibrium and thermodynamic were assessed by the concentration, time and temperature effects respectively.The thermodynamic studies suggested relatively low temperature (low energy) favoured sorption which was exothermic with a physic-sorption mechanism.

(Received July 3, 2014; September 24, 2014)

Keywords: Carbon nanotubes, Fluorine-doped,Adsorption of Cr^{3+}, Equilibrium, Thermodynamic

1. Introduction

Carbon nanotubes (CNTs) have attracted a lot of research in the past two decades due to their unique properties. These nanomaterialsareallotropes of carbon materials with a seamless tubular structure formed from sp^2hybrid C–C bonds [1, 2].They are classified into single-walled CNTs (SWCNTs) and multi-walled CNTs (MWCNTs) according to the layers of graphene sheets. CNTs have extraordinary mechanical,electricaland thermalproperties. They are often considered as one of the best candidates for the reinforcement of the next generation of multifunctional composite materials[2].

Doping of CNTs has been used in the intensive efforts devoted to developing materials with improved properties, such as high surface areas, high density of defects, and chemically active impurity sites[3-5]. Many dopants such as Nitrogen and Silicon have been used to improve CNTs properties for specific applications. The extremely high surface area-to-volume ratio makes CNTs attractive sorbent materials for the removal of pollutants from aqueous media[6, 7]. Thus, CNTs have shown good adsorption properties towards organic pollutants [8, 9],heavy metals [10-12], as well as microbes/viruses[13-15].In Nitrogen-doped CNTs, the nitrogen atoms are believed to enter the nanotube directly by substituting a carbon atom to form a three-coordinated nitrogen atom and incorporating vacancies to form a pyridine-like nitrogen atom [16]. *Ab-initio* band structure calculations for nitrogen doped carbon nanotubes showed a three coordinated nitrogen atomas an electron donor and a pyridine-like nitrogen atom as an acceptor [16]. Nitrogen doped

*Corresponding author: ezekield@vut.ac.za

carbon nanotubes yield electron-rich structures which are characterized by metallic behaviour and high density field emission current [17].

Fluorine has been used in doping CNTs[18-20]. Fluorination is an efficient method of chemically modifying CNTs because it provides the attachment of a great number of fluorine atoms to the CNT wall [16]. Fluorine-doped carbon nanomaterialshave been used for dye-sensitized solar cells [18]. An investigation of fluorine-doped CNTs as adsorbent materials is of great interest knowing that fluorine is the chemical element with the highest electronegativity value of 3.98 (on the Pauling electronegativity scale) in the periodic table.

In this study, we have synthesized fluorine-doped carbon nanotubes for the adsorption studies of chromium ions in aqueous solution. The presence of fluorine in the carbon nanotube is expected to induce high adsorption properties towards positively charged particles heavy metals like chromium in solution. To the best of our knowledge, there are no reports of fluorine-doped CNTs used as adsorbent for the removal of heavy metals, such as chromium, from aqueous medium.We herein report the synthesis and morphological characterization of fluorine doped carbon nanotubes and its utilisation as adsorbent for the removal of Cr^{3+} from aqueous solution.

2. Materials and methods

2.1 Materials

$CoSO_4$, $AgNO_3$, and NaCl(obtained from Merck) $NaHCO_3$(UnivAr), and MgO, (Sigma-Aldric) were used without modification for the preparation of cobalt and silver co-catalysts. Potassium fluoride (KF) (LabChem) was used to dope carbon nanotubes synthesized by pyrolysis of acetylene.

2.2 Preparation of cobalt and silver co-catalysts

500 ml of 1M $CoSO_4$ solution was allowed to react with 1000 ml of 1M $NaHCO_3$ solution at about 55^oC to obtain $CoCO_3$. After that, MgO (59.5g) was added to the above solution mixture containing the precipitated $CoCO_3$, the mixture was stirred for 10 min, and then filtered, thoroughly washed with distilled water, and oven dried at 70^oC for 48 h.

Also, 500ml of 1M $AgNO_3$ was allowed to react with 500ml of 1MNaCl.After that, 71.66g of MgO were added to the mixture and stir for 10 min. The mixture containing a precipitate of AgClwas then filtered, thoroughly washed with distilled water, and oven dried at 120^oC for 12 h.

The as prepared catalysts (simply referred as cobalt and silver catalyst, respectively) were grinded into very fine powder with mortar and pestle and stored for usage in the synthesis experiments.

2.3 Preparation of carbon nanotubes

The fabrication and experimental setup of this equipment have been described elsewhere [21, 22]. The fluorine-doped carbon nanotubes were synthesized by pyrolysis of acetylene gas in a tubular quartz reactor which was horizontally positioned within a furnace electronically controlled to produce accurate heating rate and reaction temperature. The bi-metallic catalyst of cobalt and silver were mixed with 2 g of KF (the dopant) and loaded into a 120 x 15 mm quartz boat at room temperature and placed in the centre of a horizontal quartz tube, which was also carefully placed in a horizontal furnace. The furnace (and its contents) was then heated while, at the same time, the flow of argon gas was commenced so as to purge the reactor of air and create an inert atmosphere for the synthesis reaction. The argon gas flow was maintained at 40 ml/min for about 70 min until the reaction temperature of 700^oC was attained. The argon gas flow rate was later increased to 240 ml/min and maintained at that flow rate (240 ml/min) for about 10 minutes to stabilize the reactor. Acetylene gas was then introduced into system at a flow rate of 50 ml/min (commencement of the synthesis reaction) and the reaction was allowed to proceed for 60 min. At the end of the reaction

period, the furnace was allowed to cool to room temperature under a continuous flow of argon gas at 40 ml/min and then,the CNTs formed inside the boat were collected.

2.4. Characterization

The structural, morphological and elemental analysis of the synthesized carbon nanotubes were carried out using Raman spectroscopy, FE-SEM, HR-TEM, EDS, and XRD. The Raman spectra were obtained by a Raman spectroscope, Jobin-Yvon HR800 UV-VIS-NIR Raman spectrometer equipped with an Olympus BX 40 attachment. The excitation wavelength was 514.5 nm with an energy setting of 1.2 mV from a coherent Innova model 308 argon-ion laser. The Raman spectra were collected by means of back scattering geometry with an acquisition time of 50 sec. The surface morphology and EDS measurements were recorded with a JEOL 7500F Field Emission scanning electron microscope. The HR-TEM images were obtained by a CM 200 electron microscope operated at 100 kV. Powder X-ray diffraction (PXRD) patterns were collected with a Bruker AXS D8 Advanced diffractometer operated at 45 kV and 40 mA with monochromated copper Kα1 radiation of wavelength (λ = 1.540598), Kα2 radiation of wavelength (λ = 1.544426),and scan speed of 1 s/step and a step size of 0.03^{o}.

2.5. Batch adsorption experiment

0.01 g of the carbon nanotube was weighed and placed in pre-cleaned test tubes. Five metal ion solutions with standard concentrations of 20, 40, 60, 80 and100 mg/l were made from spectroscopic grade standards of Cr^{3+} (from $CrCl_3$). 20 ml of each metal solution were added to each tube containing the carbon nanotube and equilibrated for 1-hour by shaking at 29^{o}C. The carbon nanotube suspensions were centrifuged for 5 min at 4000 rpm. The supernatants were analysed as stated in metal analysis.

The effect of time on adsorption was investigated as follows:0.01 g of the carbon nanotube was weighed and placed in five pre-cleaned test tubes. Metal ion solution with standard concentration of 60 mg/l was made from spectroscopic grade standard of Cr^{3+}(from $CrCl_3$). 20 ml of the metal solution was added to each tube containing the carbon nanotube and equilibrated for each time intervals of 20, 30, 40, 50 and 60 min respectively by shaking at 29^{o}C. The carbon nanotube suspensions were centrifuged for 5 min at 4000 rpm. The supernatants were analysed as stated in metal analysis.

To study the temperature effect, 0.01 g of the carbon nanotube was weighed and placed in fourpre-cleaned test tubes. Metal ion solution with standard concentrationof 60 mg/l was made from spectroscopic grade standard of Cr^{3+} (from $CrCl_3$). 20 ml of the metal solution was added to each tube containing the carbon nanotubes and equilibrated for 1-hour by shaking at temperatures of 25, 40, 60 and 80^{o}C, respectively, using a CompenstatGallenhamp water bath. The carbon nanotube suspensions were centrifuged for 5 min at 4000 rpm. The supernatants were analysed as stated in metal analysis.

The metal analysis was performed by AAS using a Buck Scientific Atomic Absorption/Emission spectrophotometer 200A (AAES), with the following parameters: Lamp current: 10 mA, λ: 357.9 nm, Slit width: 0.7 nm, Fuel gas flow rate: 15.0 L/min, Burner height: 9.0 mm,Flame type: air-acetylene. Controls of one of the metal solution were run to detect any possible metal precipitation or contamination**.**

For data analysis,various equilibrium, kinetic, and thermodynamic models (equations) were employed to interpret the data and establish the extent of adsorption. The amount of metal uptake was computed using the material balance equation for batch dynamic studies (equation 1)[23].

$$q_e = \frac{V}{M}(C_o - C_e) \tag{1}$$

withq_e is metal uptake capacity (*mg/g*carbon nanotube at equilibrium), $C_e$is metal ion concentration in solution (*mg/g*) at equilibrium, C_o is the initial metal ion solution (*mg/g*), *V* is the volume of solution in litres and*M*, the dry weight of carbon nanotube used in (*g*).

Langmuir plots were carried out using the linearized equation 2 below

$$\frac{M}{X} = \frac{1}{abC_e} + \frac{1}{b} \tag{2}$$

Where$X$ is the amount of Cr^{3+} adsorbed per mass M of carbon nanotube inmg/g, a and$b$ are the Langmuir constants obtained from the slope and intercepts of the plots.

The essential characteristics of the Langmuir isotherm were expressed in terms of a dimensionless separation factor or equilibrium parameterS_f[24].

$$S_f = \frac{1}{(1+aC_o)} \tag{3}$$

WithC_o as initial concentration of Cr^{3+} in solution, the magnitude of the parameterS_f provides a measure of the type of adsorption isotherm. IfS_f> 1.0, the isotherm is unfavourable;S_f = 1.0 (linear); 0<S_f< 1.0(favourable) and S_f=0 (irreversible).

The adsorption intensity of the Cr^{3+} in the carbon nanotube was assessed from the Freundlich[25] plots using the linearized equation 4 below

$$ln\frac{X}{M} = \frac{1}{n}(lnC_e) + lnK \tag{4}$$

Where$K$ and$n$ are Freundlich constants and 1/n is approximately equal to the adsorption capacity.
The fraction of carbon nanotube surface covered [26, 27] by the Cr^{3+} was computed using equation 5

$$\theta = 1 - \frac{C_e}{C_o} \tag{5}$$

With θ as degree of surface coverage

The effectiveness of the adsorbent (CNTs) was assessed by the number of cycles of equilibrium sorption process required to reduce the levels of Cr^{3+} in solution according to the value of the distribution (partition coefficient (K_d) [28] in equation 6.

$$K_d = \frac{C_{aq}}{C_{ads}} \tag{6}$$

Where$C_{aq}$is concentration of Cr^{3+} (mg/g)in solution; C_{ads} is concentration of Cr^{3+}(mg/l)in CNTs.
The heat of adsorption (Q_{ads}) was obtained using the following Suzuki equation.

$$ln\theta = \frac{lnK_oC_o}{T^{0.5}} + \frac{Q_{ads}}{RT} \tag{7}$$

With$T$ as solution temperature (K);K_o a constant and R gas constant (8.314 J/K.mol).
The linear form of the modified Arrhenius expression was applied to the experimental data to evaluate the activation energy (E_a) and sticking probability S* as shown in equation 8.

$$ln(1-\theta) = S^* + \frac{E_a}{RT} \tag{8}$$

The apparent Gibbs free energy of sorption ΔG^owhich is a fundamental criterion for spontaneity, was evaluated using the following equation

$$\Delta G^o = -RTlnK_o \tag{9}$$

$K_o$is obtained from the Suzuki equation (Eq. 7).

The experimental data was further subjected to thermodynamic treatment in order to evaluate the apparent enthalpy ($\Delta H°$) and entropy ($\Delta S°$) of sorption using equation 10.

$$lnK_o = \frac{\Delta S^o}{R} - \frac{\Delta H^o}{RT} \tag{10}$$

The expression relating the number of hopping (n) and that of the surface coverage (θ) as shown in equation 11 was applied to the experimental data.

$$n = \frac{1}{(1-\theta)\theta} \tag{11}$$

WithC_o andC_e as initial and equilibrium concentrations inmol/cm^3;R, the gas constant and$T$, the solution temperature in K

3. Results and discussion

3.1 SEM and TEM

Scanning and transmission electron microscopy images of fluorine doped carbon nanomaterial are presented in figures 1 and 2. In order to determine the morphology of the carbon nanotubes, scanning electron microscope (SEM), and transmission electron microscope (TEM) images of the sample were taken at a magnification of x270. The SEM and TEM images show that the surface of CNTs had irregular small size particles which indicated a high surface area and porous nature as shown in figures 1 and 2. Large surface area of any adsorbent facilitates maximum adsorption.

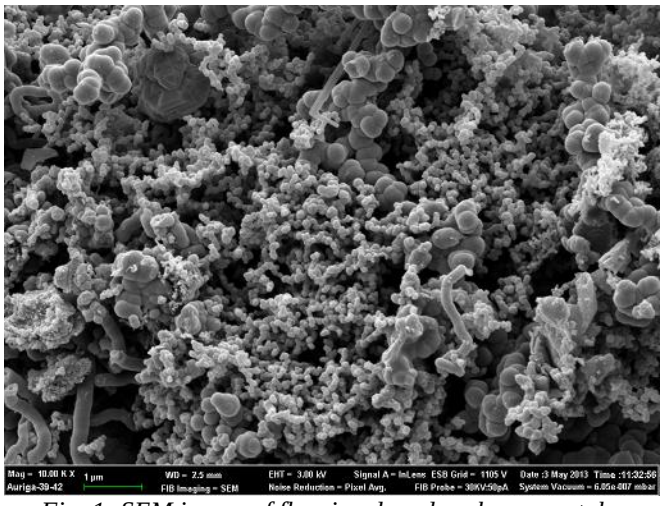

Fig. 1: SEM image of fluorine doped carbon nanotube

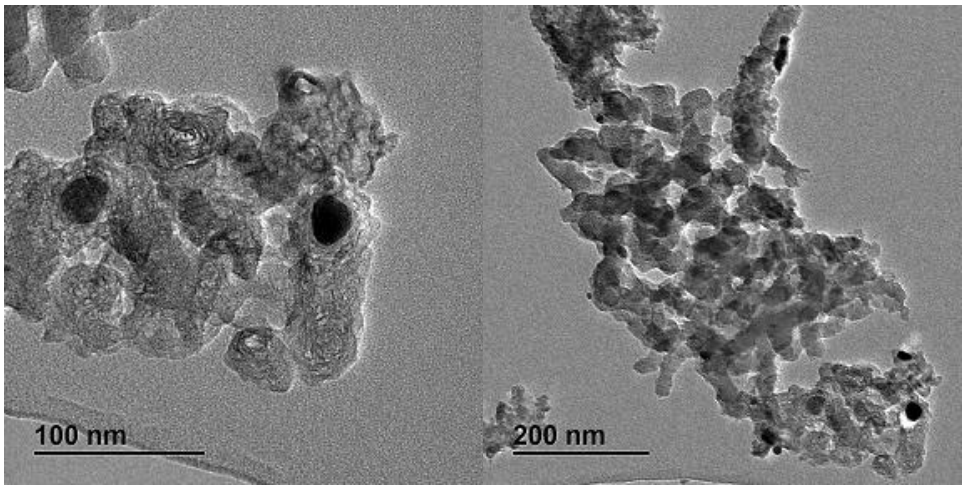

Fig. 2: TEM images of fluorine doped carbon nanotube

3.2 Raman study

Generally, Raman spectral showed two major peaks of D and G bands appearing at around 1340 and 1580 cm^{-1}, deriving from in-plane motion of the carbon atoms to provide a signature of carbon nanotubes ([29]. Berciaud*et al*. [30] reported that the Raman spectral signature of carbon nanotubes is very sensitive to strain effects as well as doping. The Raman spectral feature of fluorine-doped carbon nanotubes (Figure 3) has two major peaks at 1340 and 1596 cm^{-1}. The appearance of these bands in the Raman spectral of our fluorine-doped carbon nanotubes, assigned to the G (1596 cm^{-1}) and D (1340 cm^{-1}) band shifted because of the doping effect of fluorine. The obtained Raman spectral feature could be assigned to the multiwall nanotube because of the absence (weakness) of radial breathing mode (RBM) which normally appears between 120 and 250 cm^{-1} in single wall nanotubes ([29, 31]. Ferrari [32] attributed these G and D peaks to sp^2 sites of the carbon based materials.

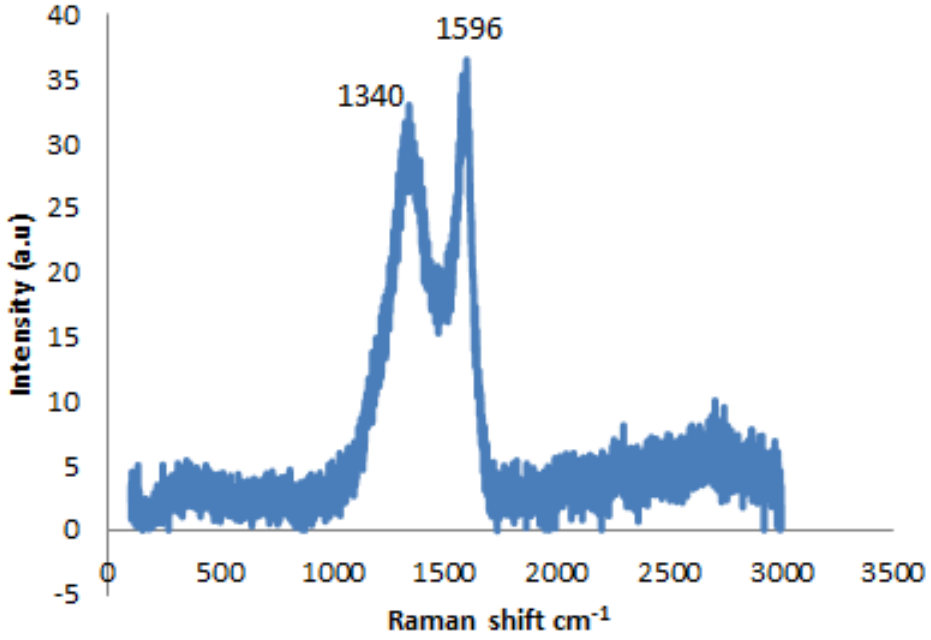

Fig. 3: Raman spectra of fluorine doped carbon nanotubes

3.3 EDS analysis

Energy dispersive X-ray spectroscopy (EDS) was used for elemental analysis of the fluorine-doped CNTs. The EDX spectrum in figure 4 confirmed the presence of the carbon atom (intense peak), the dopant F, and component of the catalysts (Na, Mg, Ag, K) in trace quantities. The presence of these elements will produce charges on the surface of the nanotubes and create electrostatic forces of attraction between the sample and Cr^{3+} in solution.

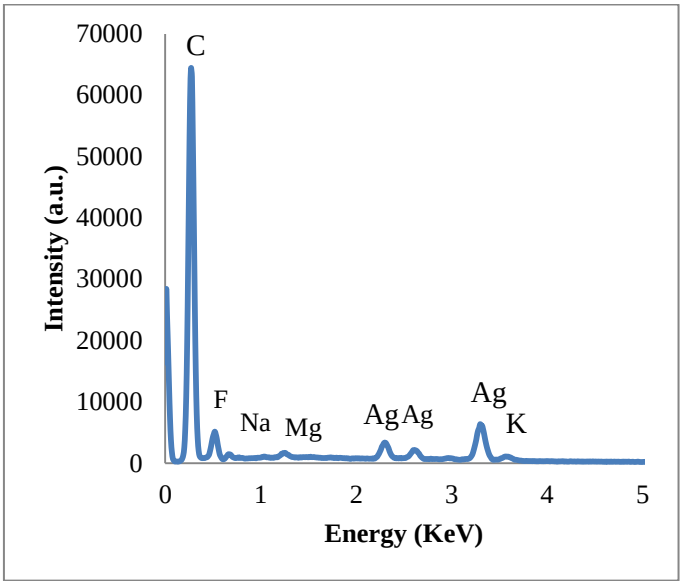

Fig. 4: Energy dispersive X-ray spectroscopy (EDS) spectra of fluorine doped carbonnanotube

3.4 XRD results

X-ray diffraction, as a powerful tool for characterizing solid state samples, provides specific crystalline pattern for each substance. This technique was used to characterize the fluorine-doped CNTs and the result is presented in Figure 5. The XRD patterns of fluorine-doped CNTs shows major peaks at around 2θ = 24 and 44°. These peaks were attributed to the hexagonal graphite structures (0 0 2) and (1 0 0), respectively. Therefore, the as-grown CNTs are assumed to be amorphous, as also revealed by the SEM and TEM images. Similar results have been reported by Ci*et al*. [33] (who called their product amorphous CNTs) and Li *et al*. [34]. No explanation related to the small and sharp peak around 2θ = 31° could be found in the literature. However, we assumed that this peak could be attributed to the crystalline region of fluorine-doped CNTs.

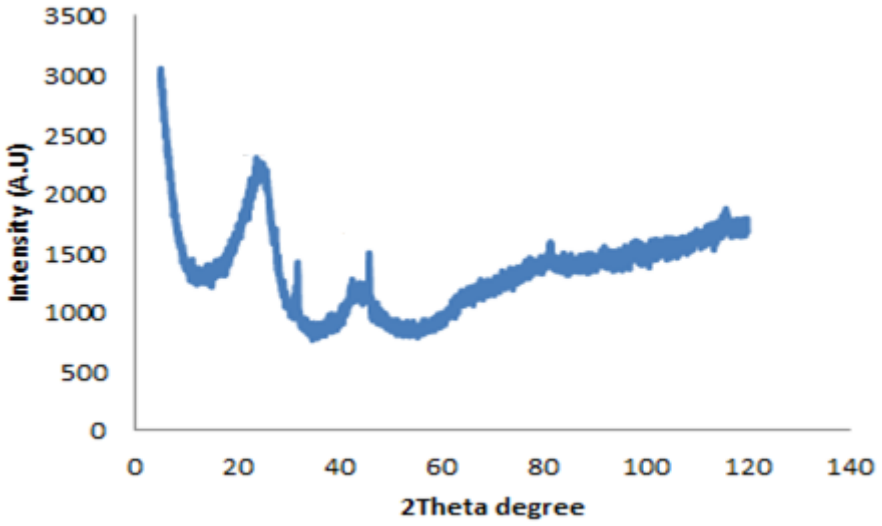

Fig. 5: X-ray diffraction analysis of fluorine doped carbon nanotube

3.5 Adsorption study

Effect of concentration: The percentage sorption of Cr^{3+} by theCNTs at different concentrations of the Cr^{3+} is presented in figure 6. The maximum adsorption of 60% took place at equilibrium concentration of 20mg/l Cr^{3+}. This is because at lower concentration more nanotubes pore spaces were available for the Cr^{3+}, but as the concentration of Cr^{3+} increased, the adsorption capacity of the CNTs decreased due to reduced availability of free pore spaces. The results indicated that the sorption of Cr^{3+} were very much dependent on the concentration of the Cr^{3+}.

Time dependency: Time dependency studies show the amount of time needed for maximum adsorption to occur. The variation in percentage removal of Cr^{3+} with time has been presented in figure 6. It indicates that a maximum of 65% removal of Cr^{3+} was observedin 20 minutes and remained constant afterwards. The relatively short contact time required to attain equilibrium suggests that a rapid uptake of Cr^{3+} by the nanotubes occurred to fill some of the vacant pores in the CNTs and after which the remaining spaces were difficult to be occupied due to repulsive forces between the Cr ions.

Effect of temperature: Figure 6 also presents the plot of percentage adsorption of $Cr^{3+}$by the carbon nanotubes at varying temperatures with optimum sorption of 50% occurring at 28^{o}C. The plot showed that further increase in temperature resulted in a slight decrease in adsorption. This is in agreement with the general principle that physical adsorption decreases with increase in temperature [35, 36]. This behaviour could be attributed to the weakening of the attractive forces between the nanotubes and Cr^{3+}, the increased kinetic energy of the Cr^{3+} and the decrease in the thickness of the boundary layers of the carbon nanotube due to the higher tendency of the Cr^{3+} to escape from the pores.

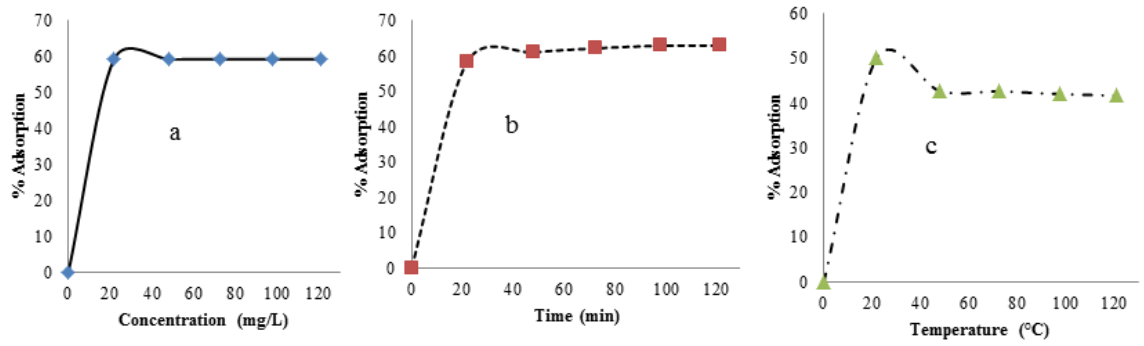

Fig. 6: Adsorption efficiency of carbon nanotubewith Cr^{3+} at (a) concentration, (b) Time and (c) Temperature

Adsorption isotherms: The extent of adsorption can be correlated by means of an isotherm. Attempts were made to fit the data obtained from the adsorption experiments into various adsorption isotherms. The linear plots of the Langmuir and Freundlich isotherm models for the sorption of Cr^{3+} by the carbon nanotubes are presented in figure 7. These straight line plots confirmed the application of the Langmuir and Freundlich isotherm models to the adsorption of Cr^{3+} by the nanotubes. The slopes and intercepts were used to compute the Langmuir constants and adsorption capacity.

The fraction of the CNTs surface covered by the Cr^{3+} is givenas 0.63 (Table 1). This value indicates that 63% of the pore spaces of the nanotubes surface were covered by the Cr^{3+}, which means high degree of adsorption.

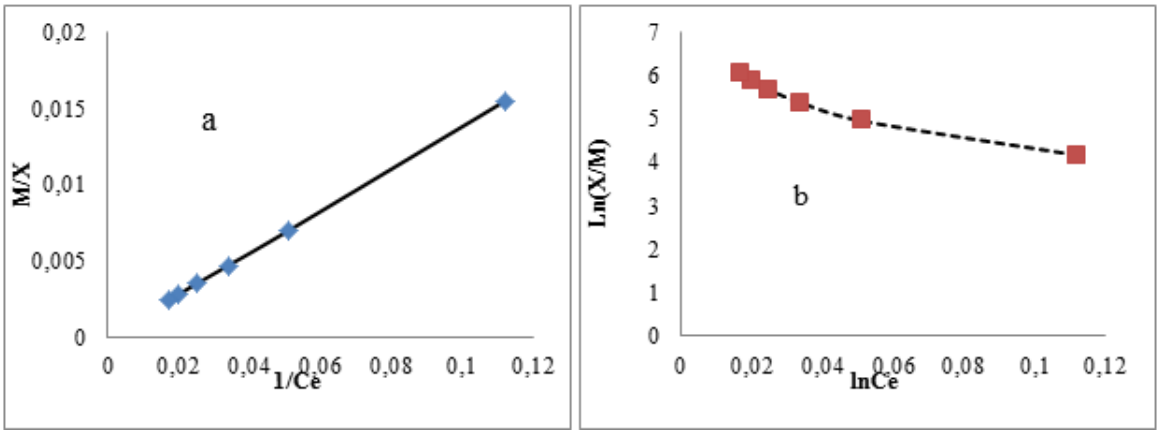

Fig. 7: Equilibrium plots of adsorption of Cr^{3+} on polystyrene waste, (a) Langmuir and (b) Freundlich

Table 1: Equilibrium and thermodynamic parameters

Heat of adsorption Q_{ads} *KJ/molK*	Sticking probability S*	Activation energy E_a *J/molK*	Gibbs free energy of adsorption $\Delta G°$ *KJ/mol*	Apparent entropy $\Delta S°$ *J/molK*	Apparent enthalpy $\Delta H°$ *J/mol*	Surface coverage θ	Separation factor S_f	Hopping number n	Sorption coefficient K_d
-1.34	0.719	-162.0	-0.770	1.670	-160.9	0.630	0.677	4	0.474

In order to determine the nature of the adsorption process, whether favourable or unfavourable, the dimensionless constant separation termS_f was investigated (equation 3). The result (S_f=0.677) in Table 1 was less than one and greater than zero which showed that the sorption of Cr^{3+} onto the carbon nanotube was favourable.

The effectiveness of the CNTs as adsorbent for Cr^{3+} from solution was assessed through the sorption distribution or partition coefficientK_d presented in Table 1. The value ofK_d(0.474) suggests that CNTsare an effective adsorbent and that a very few number of cycles of equilibrium sorption process will be required to reduce the levels of Cr^{3+} in solution.

In order to calculate the heat of adsorption (Q_{ads}) for the sorption of Cr^{3+} onto the CNTs, equation 7 was used. The value of Q_{ads} (-1.34 $KJmol^{-1}K^{-1}$) is negative as presented in Table 1, which indicates that the adsorption was exothermic i.e. low temperatures favour the adsorption of Cr^{3+} by the nanotube. Temperature increase did not enhance the sorption process.

The activation energy $E_a$and the sticking probability S* were calculated from equation 8. The value of E_a and S* were shown in Table 1 as -162.0 $Jk^{-1}mol^{-1}$ and 0.719, respectively. The relatively low and negative E_a value indicates that low temperature or energy favours the sorption and the adsorption process is exothermic. Relatively low value of E_a also suggests that the sorption process is diffusion controlled. The sticking probability S* indicates the measure of the potential of an adsorbate to remain on the adsorbent. It is often interpreted as S*> 1 (no sorption), S*= 1 (mixture of physic-sorption and chemisorption), S* = 0 (indefinite sticking – chemisorption), 0<S*<1 (favourable sticking – physic-sorption). The value of S* obtained for the sorption of Cr^{3+} by the CNTs was between zero and one which indicates that the adsorption was favourable and followed physic-sorption mechanism.

Table 1 also presents the Gibbs free energy ΔG^o for the sorption of Cr^{3+} by the CNTs which was calculated from equation 9. Gibbs free energy is the fundamental criterion of spontaneity. The ΔG^ovalue of -0.770 KJ/mol was negative indicating that the sorption process was spontaneous. The value obtained for ΔG^o was also less than -20KJ/mol suggesting

electrostatic interaction between the Cr^{3+} and the nanotube which supported physic-sorption mechanism.

The values of the enthalpy change (ΔH^o) and entropy change ΔSwere calculated from equation 10 to be -160.9 J/mol and 1.67 $J/molK$respectively. A negative ΔH^o suggests that sorption proceeded favourably at a lower temperature and the sorption mechanism was exothermic. A positive ΔS suggests that the freedom of the adsorbed Cr^{3+} was not restricted in the carbon nanotubes, indicating that physic-sorption mechanism predominates.

The probability of Cr^{3+} finding vacant site on the surface of the carbon nanotube during the sorption was correlated by the number of hopping (n) done by the Cr^{3+}. The hopping number presented in Table 1 is 4(the lower the hopping number, the faster the adsorption[35, 37]). The low value of *n* obtained in this study suggests that the adsorption of Cr^{3+} on the nanotubes was very fast.

4. Conclusion

Fluorine-doped CNTs were successfully synthesized and the results of the characterization confirmed amorphous multiwall carbon nanotubes with some crystalline regions due to the doping with fluorine. The equilibrium and thermodynamic batch adsorption studies recorded rapid uptake of the Cr^{3+} by the CNTs which was diffusion controlled. The adsorption was favoured by low temperature and energy which was exothermic with a physic-sorption mechanism. The results from this study will add to the knowledge base on the synthesis, characterization and the use of nanotubes for the sorption of metal ions from aqueous solutions.

Acknowledgement

This work was supported by a research grant from the Research Directorate of the Vaal University of Technology/ Vanderbijlpark, South Africa.

References

[1] C. Li, G. Shi, J. Photochem. Photobiol.**19**, 20 (2014)
[2] X. Wang, P. D. Bradford, Q. Y.Li, Zhu, J. Mark, N. Schulz-Vesselin, Z. Y. Shanov, (ed.), Nanotube Superfiber Mat., 649 (2014)
[3] E.N. Nxumalo, N.J.Coville, Materials, **3(3)** 2141 (2010)
[4] Z. Pu, Q. Liu, C. Tang, A.M. Asiri, A.H. Qusti, A.O. Al-Youbi, X.Sun, J. Power Sources **257**, 170 (2014)
[5] W.Y. Wong, W. R. W. Daud, A. B. Mohamad, A. A. H.Kadhum, K. S. Loh, E. H. Majlan, K. L. Lim,Electrochim. Acta, **129**, 47 (2014)
[6] M.J., Gallagher, H., Huang, K.J. Schwab, D.H.Fairbrother,Teychene, B. J. Membr. Sci., **446**, 59 (2013)
[7] H. Wei, S. Deng, Q.Huang, Y. Nie, B. Wang, J.Huang, G.Yu,Water Res. **47(12),** 4139 (2013)
[8] C.D.Vecitis,G. D.Gao, H. Liu, J. Phys. Chem. C. **115(9),** 3621 (2011)
[9] H. Li, X. Gui, L. Zhang, S. Wang, C. Ji, J. Wei, K. Wang, H. Zhu, D. Wu, A. Cao,Chem. Commun.,**46,** 7966 (2010)
[10] T. Mohammadi, M.A. Tofighy,J. Hazard. Mater.,**185**, 140 (2011)
[11] O. Moradi,K.Zare,M.Monajjemi,M.Yari, H. Aghaie,Fullerenes, Nanotubes Carbon Nanostructures, **18(3)**, 285 (2010)
[12] D.S. Su, Y.J. Xu, R. Arrigo, X. Liu, New Carbon Mater, **26,** 57 (2011)
[13] A.S. Brady-Estévez, T.H. Nguyen, L. Gutierrez, M. Elimelech, Water Res., **44**, 3773 (2010)
[14] S.T. Mostafavi, M.R. Mehrnia, A.M. Rashidi, Desalination, **238**, 271 (2009)
[15]S. Kang, M.S. Mauter, M. Elimelech,Environ. Sci. Technol., **43,** 2648 (2009)

[16] L. G. Bulusheva, A. V. Okotrub, A. G. Kudashov, N. F. Yudanov, E. M. Pazhetnov, A. I. Boronin, O. G. Abrosimov, N. A. Rudina, Russ. J. Inorg. Chem. **51(4)** 613 (2006).
[17] A. V. Okotrub, N. Maksimova, T. A. Duda, A. G. Kudashov, Yu. V. Shubin, D. S. Su, E. M. Pazhetnov, A. I. Boronin, L. G. Bulusheva, Fullerenes, Nanotubes Carbon Nanostructures, **12,** 99 (2004)
[18] T.I. Jeona, J.H. Son, K.H. An, Y.H. Lee, Y.S. Lee,J. Appl. Phys., **98,** 034316 (2005)
[19] M. K.Seo, S.J. Park,Bull. Korean Chem. Soc., **30(9),** 2071 (2009)
[20] A.Capasso, L.Salamandra, A.Chou, A.D.Carlo, N.Motta,Sol. Energy Mater. Sol. Cells., **122,** 297 (2014)
[21] T. Ebbensen, A. Ajayan, H. Huira, K. Tanigaki, Nature, 367, (1994)
[22] A.S.Afolabi, A.S. Abdulkareem, S.D. Mhlanga, S.E.Iyuke, J. Expt. Nanoscience, **6**(3), 248 (2011)
[23] K. H. Chu, M.A. Hashim, ActaBiotechnol., **21**(4), 295 (2001)
[24] V.J.P. Poots, G. McKay, J.J. Healy, J. Water Pollut. Control Fed. **50(5)**, 926 (1978)
[25] K.Y. Shin, J.Y. Hong, J. Jang, J. Hazard. Mater.,**190,** 36 (2011)
[26] E. L. K.Mui, W. H.Cheunga, M.Valix, G. McKay, J. Colloid Interface Sci.,**347**, 290 (2010)
[27] Y.Lipatov, V.Chornaya, T.Todosijchuk, G. Menzheres, J. Colloid. Surf. Sci., **294,** 273 (2006)
[28] C.-Y.Zhanga, H.-C.Hua,X.-S.Chaia,L.Panb, X.-M. Xiao, J. Chromatogr. A, **1310**, 121 (2013)
[29] A.Jorio,M. A.Pimenta,A. G. Souza Filho,R. Saito, G. Dresselhaus, M.S. Dresselhaus, New J. Phys., **5,** 139.1 (2003)
[30] S.Berciaud,S.Ryu,L. E.Brus, T.F. Heinz, Nano Lett., **9(1),** 246 (2009)
[31] M. S.Dresselhaus,G.Dresselhaus, R. Saito, A. Jorio, Phys. Reports, **409,** 47 (2005)
[32] A.C. Ferrari,Mater. Res. Soc. Sympos.Proceed, 675. (2001)
[33] L.Ci,B. Wei,C.Xu,J. Liang,D. Wu,S.Xie,W. Zhou,Y. Li,Z. Liu, D. Tang, J. Cryst. Growth, **233**, 823 (2001)
[34] W. Li,C. Liang,W. Zhou,J.Qiu, Z. Zhou, G. Sun, Q. Xin, J. Phys. Chem. B, **107(26),** 6292 (2003)
[35] D. Wankasi, E. D. Dikio, J. Chem., doi:.org/10.1155/817527 (2014)
[36] S. Al-Asheh, Z. Duvnjak,Biotechnol. Progr.**11(6),** 638 (1995)
[37] M. C.Menkiti,M. C.Aneke,P. M.Ejikeme, O.D. Onukwuli, N.U. Menketi,SpringerPlus, **3(213),** 1 (2014)